The CC Chemokine Thymus-derived Chemotactic Agent 4 (TCA-4, Secondary Lymphoid Tissue Chemokine, 6Ckine, Exodus-2) Triggers Lymphocyte Function–associated Antigen 1–mediated Arrest of Rolling T Lymphocytes in Peripheral Lymph Node High Endothelial Venules✪

By Jens V. Stein,* Antal Rot,‖ Yi Luo,‡ Manjunath Narasimhaswamy,* Hideki Nakano,¶ Michael D. Gunn,** Akio Matsuzawa,‡‡ Elizabeth J. Quackenbush,*§ Martin E. Dorf,‡ and Ulrich H. von Andrian*‡

*From *The Center for Blood Research, the ‡Department of Pathology, and the §Children's Hospital, Harvard Medical School, Boston, Massachusetts 02115; ‖Novartis Forschungsinstitut, A-1235 Vienna, Austria; the ¶Department of Immunology, Toho University School of Medicine, Tokyo 143-8540, Japan; the **Division of Cardiology, Duke University Medical Center, Durham, North Carolina 27710; and the ‡‡Institute of Medical Science, University of Tokyo, Tokyo 108-8639, Japan*

Abstract

T cell homing to peripheral lymph nodes (PLNs) is defined by a multistep sequence of interactions between lymphocytes and endothelial cells in high endothelial venules (HEVs). After initial tethering and rolling via L-selectin, firm adhesion of T cells requires rapid upregulation of lymphocyte function–associated antigen 1 (LFA-1) adhesiveness by a previously unknown pathway that activates a $G\alpha_i$-linked receptor. Here, we used intravital microscopy of murine PLNs to study the role of thymus-derived chemotactic agent (TCA)-4 (secondary lymphoid tissue chemokine, 6Ckine, Exodus-2) in homing of adoptively transferred T cells from T-GFP mice, a transgenic strain that expresses green fluorescent protein (GFP) selectively in naive T lymphocytes (T^{GFP} cells). TCA-4 was constitutively presented on the luminal surface of HEVs, where it was required for LFA-1 activation on rolling T^{GFP} cells. Desensitization of the TCA-4 receptor, CC chemokine receptor 7 (CCR7), blocked T^{GFP} cell adherence in wild-type HEVs, whereas desensitization to stromal cell–derived factor (SDF)-1α (the ligand for CXC chemokine receptor 4 [CXCR4]) did not affect T^{GFP} cell behavior. TCA-4 protein was not detected on the luminal surface of PLN HEVs in *plt/plt* mice, which have a congenital defect in T cell homing to PLNs. Accordingly, T^{GFP} cells rolled but did not arrest in *plt/plt* HEVs. When TCA-4 was injected intracutaneously into *plt/plt* mice, the chemokine entered afferent lymph vessels and accumulated in draining PLNs. 2 h after intracutaneous injection, luminal presentation of TCA-4 was detectable in a subset of HEVs, and LFA-1–mediated T^{GFP} cell adhesion was restored in these vessels. We conclude that TCA-4 is both required and sufficient for LFA-1 activation on rolling T cells in PLN HEVs. This study also highlights a hitherto undocumented role for chemokines contained in afferent lymph, which may modulate leukocyte recruitment in draining PLNs.

Key words: homing • intravital microscopy • adhesion • T cell

Introduction

T lymphocytes continuously recirculate through the body, traveling from the blood through tissues, and via lymphatic vessels and the thoracic duct back into the blood (1–3). Secondary lymphoid organs, such as spleen, peripheral LNs (PLNs),[1] mesenteric LNs (MLNs), and Peyer's patches (PPs)

✪The online version of this article contains supplemental material.

Address correspondence to U.H. von Andrian, The Center for Blood Research and Department of Pathology, Harvard Medical School, 200 Longwood Ave., Boston, MA 02115. Phone: 617-278-3130; Fax: 617-278-3190; E-mail: uva@cbr.med.harvard.edu

[1]*Abbreviations used in this paper:* CCR, CC chemokine receptor; CXCR, CXC chemokine receptor; DC, dendritic cell; DNP, dinitrophenol; EC, endothelial cell; GFP, green fluorescent protein; HEV, high endothelial venule; MIP, macrophage inflammatory protein; MLN, mesenteric LN; PLN, peripheral LN; *plt*, paucity in LN T cells; PNAd, peripheral node addressin; PP, Peyer's patch; PTX, pertussis toxin; SDF, stromal cell–derived factor; TCA, thymus-derived chemotactic agent.

Downloaded from http://rupress.org/jem/article-pdf/191/1/61/1123529/99-0903.pdf by guest on 24 May 2022

are sites of intense lymphocyte trafficking. Tissue-specific homing of blood-borne naive lymphocytes into secondary lymphoid tissues is critical to ensure frequent and efficient encounters between APCs and antigen-specific T cells (3, 4).

The cutaneous hypersensitivity reaction is a good example for illustrating the importance of T cell homing to PLNs. In this setting, antigen that penetrates the skin is taken up by Langerhans cells. Subsequently, these professional APCs enter afferent lymph vessels, which channel cells and interstitial fluid to local PLNs (4). The antigen-laden APCs then induce the activation, expansion, and differentiation of antigen-specific T cells that must enter skin-draining PLNs from the blood. Within a few days, primed T cells leave the PLNs and migrate to the skin. Upon renewed cutaneous exposure to antigen, these cells mediate a local inflammatory (delayed-type hypersensitivity) response. This sequence is disrupted in L-selectin (CD62L)-deficient mice, because their T cells cannot home to PLNs where antigen is presented (5). Thus, L-selectin–deficient animals respond poorly to cutaneous antigen unless T cell homing to PLNs is temporarily restored (5, 6).

Recently, the adhesion cascade that governs lymphocyte homing to PLNs has been partially elucidated (7). Circulating lymphocytes must first adhere to microvascular endothelial cells (ECs) in the presence of hydrodynamic shear exerted by the flowing blood. An initial tether is formed by L-selectin, which binds to the peripheral node addressin (PNAd), a mixture of sialylated, fucosylated, and sulfated glycoproteins that are selectively expressed in specialized postcapillary microvessels, the high endothelial venules (HEVs) (8, 9). L-selectin interaction with PNAd allows lymphocytes to roll in HEVs at a velocity that is much slower than that of noninteracting cells (10). Within seconds after initial contact, a fraction ($\sim$20–30%) of rolling lymphocytes arrest firmly ("stick"), a process that requires the β2-integrin LFA-1 (CD11a/CD18) (7). The sequential engagement of L-selectin and LFA-1 is a prerequisite for subsequent extravasation of lymphocytes in PLNs (11–15).

However, expression of L-selectin and LFA-1 alone is not sufficient for homing to PLNs. Both are abundantly expressed on other leukocytes, including granulocytes, which do not home to PLNs. Granulocytes undergo L-selectin–mediated rolling interactions in PLN HEVs, but they do not stick (7). A likely explanation for this observation is the fact that L-selectin binding to PNAd is independent of a cell's activation state, whereas LFA-1 must be functionally activated (16). The intracellular events that lead to LFA-1 activation are believed to be triggered by chemoattractant receptors on the lymphocyte surface. Accordingly, LFA-1 activation in PLN HEVs is blocked by pertussis toxin (PTX)-mediated ADP-ribosylation of $G\alpha_i$, the regulatory subunit of large heterotrimeric G proteins. Pretreatment of lymphocytes with PTX abrogates LFA-1–dependent sticking in PLN HEVs (7, 17). Thus, it has been hypothesized that LFA-1 activation requires stimulation of a G protein–coupled receptor that is expressed on lymphocytes, but not granulocytes (2, 3, 7). Chemokines are likely candidates to provide such a stimulus, as they bind $G\alpha_i$-linked receptors whose expression is often restricted to distinct leukocyte subsets (18, 19).

Several chemokines possess potent and selective chemoattractant activity for naive lymphocytes (19). One of these is thymus-derived chemotactic agent (TCA)-4 (secondary lymphoid-tissue chemokine [SLC], 6Ckine, or Exodus-2), a CC chemokine that acts on lymphocytes, dendritic cells (DCs), and mesangial cells, but not on monocytes or granulocytes (20–23). In chemotaxis assays, TCA-4 attracts T and B cells; its chemoattractant potency is somewhat higher on naive than memory T cells (20–24). CC chemokine receptor (CCR)7, the principal TCA-4 receptor (24, 25), is expressed on lymphocytes and DCs, but not on granulocytes and monocytes (26, 27). In addition to inducing lymphocyte chemotaxis over a time course of minutes to hours, in vitro experiments have shown that TCA-4 can also trigger much more rapid (within seconds or less) integrin binding to immobilized intracellular adhesion molecule (ICAM)-1 and mucosal addressin cell adhesion molecule (MAdCAM)-1 under both static and flow conditions (28–30). Studies by several groups using immunohistology, Northern blots, and in situ hybridization have shown that TCA-4 is constitutively expressed in secondary lymphoid organs and in lymph vessels (20–23). The highest mRNA levels were seen in the T cell area of PLNs, particularly in HEVs (22). Thus, TCA-4 meets several requirements for a chemoattractant that might activate LFA-1 on rolling lymphocytes in PLNs: (a) its receptor, CCR7, is expressed on naive T cells, the predominant PLN-tropic lymphocyte population; (b) CCR7 activation triggers a rapid integrin response; and (c) TCA-4 is expressed in HEVs, the main port of lymphocyte entry into PLNs.

Recent experiments in DDD/1-*plt/plt* (*plt/plt*) mice further implicate TCA-4 in T cell homing. These mice have an autosomal recessive gene defect termed *plt* (paucity in LN T cells). Their PLNs contain few T cells, but normal numbers of B cells (31). The few T cells that are present in *plt/plt* PLNs belong to the memory subset, whereas wild-type PLNs contain mostly naive T cells (32). Homozygous *plt/plt* mice have elevated T cell numbers in blood and spleen, suggesting a selective defect in naive T cell homing to PLNs. This defect appears to be localized in the PLN stroma, since adoptively transferred *plt/plt* T cells home normally to PLNs of wild-type mice, whereas wild-type T cells home poorly to *plt/plt* PLNs (31, 32). Moreover, B cell homing to PLNs is essentially normal in *plt/plt* mice, indicating that the homing defect is not due to a lack of endothelial adhesion molecules (31). Indeed, a recent report has found that TCA-4 mRNA is absent in PLNs of these mice (33). However, the available data do not exclude the possibility that the *plt* mutation affects other genes that could be required for T cell homing independent of TCA-4. Moreover, it has not been determined whether TCA-4 protein is absent in *plt/plt* PLNs. Conceivably, TCA-4 might be produced in nonlymphoid tissues of *plt/plt* mice, from where it could be drained into PLNs via afferent lymph vessels.

Finally, in addition to TCA-4, other chemokines are present in PLNs that can also activate integrins on rolling T

Downloaded from http://rupress.org/jem/article-pdf/191/1/61/1123529/99-0903.pdf by guest on 24 May 2022

cells in vitro (28). However, this constitutes no proof that TCA-4 or other chemokines are indeed involved in integrin activation in HEVs, because chemoattractants must be present on the luminal surface of HEVs. To date, no unequivocal evidence has been presented for the presence of a chemokine in this microanatomical location. Thus, a direct role for TCA-4 or any other chemokine in the multistep adhesion cascade of lymphocyte homing in HEVs remains to be documented.

Here, we used intravital microscopy to investigate the physiological role of TCA-4 in T cell homing to PLNs. TCA-4 was concentrated on the luminal surface of wild-type, but not *plt/plt* PLN HEVs. To study the effect of TCA-4 specifically on T cells, we made use of a novel strain of transgenic (T-GFP) mice, which express green fluorescent protein (GFP) under a T cell–specific promoter. Adoptively transferred naive T lymphocytes (T^{GFP} cells) from T-GFP mice were visualized in PLN HEVs of wild-type and *plt/plt* mice by epifluorescence illumination. When T^{GFP} cells were desensitized to TCA-4, they failed to stick in wild-type PLNs, whereas desensitization to another chemokine, stromal cell–derived factor (SDF)-1α, had no effect. Upon injection into *plt/plt* mice, T^{GFP} cells rolled in PLN HEVs, but did not stick. This defect in *plt/plt* mice was reversed after intracutaneous injection of TCA-4. The injected chemokine accumulated rapidly in draining PLNs and was detectable in a subpopulation of HEVs where it reconstituted LFA-1–mediated sticking of T^{GFP} cells. These results document a central role for TCA-4 in the subset- and tissue-specific adhesion cascade that mediates T cell homing to PLNs.

Materials and Methods

Antibodies and Reagents. Anti-PNAd mAb MECA-79 (rat IgM [9]) and anti–murine TCA-4 mAbs 4B1 and 3D5 (Armenian hamster IgG [20]) were generated from culture supernatants. Anti–mouse LFA-1 mAb TIB 213 (rat IgG2b [34]), FITC-conjugated anti–murine TCA-4 mAb 4B1 (specific fluorescence to protein [F/P; mol/mol] ratio 3.74), and FITC-conjugated anti-dinitrophenol (DNP) mAb (specific F/P ratio 4.20; Armenian hamster IgG) used as nonbinding control were provided by Dr. Eugene Butcher (Stanford University, Stanford, CA). Anti–mouse CD16/CD32, PE-conjugated B220, and PE-conjugated CD3 mAbs were from PharMingen. Recombinant murine TCA-4 and human SDF-1α were from R&D Systems. For some experiments, we used full-length and COOH-terminally truncated murine TCA-4 prepared using the His-patched thioredoxin fusion protein method (20). Activity of full-length TCA-4 from both sources was indistinguishable in chemotaxis and calcium flux assays (not shown). Truncated TCA-4 (TCA-$4_{\Delta CT}$) was generated by introducing a stop codon after amino acid Q69 (20). Thus, recombinant TCA-$4_{\Delta CT}$ lacked the last 41 amino acids of the elongated COOH terminus (20–23). Human ^{125}I–TCA-4 (96 mCi/mg) was a gift of Dr. Diane True (New England Nuclear, Boston, MA). FITC-dextran (150 kD) was purchased from Sigma Chemical Co. Before injection into animals, FITC-dextran was dissolved in sterile saline (10 mg/ml) and centrifuged to remove insoluble particles.

Mice. *plt/plt* mice on DDD/1 background (31, 32) were used for intravital microscopy and as organ donors for most immunohistology studies. DDD/1–*mtv-2/mtv-2* mice served as wild-type controls (31). BALB/c mice (Charles River) were used to measure kinetics of intracutaneously injected TCA-4. BALB/c mice (The Jackson Laboratory) were also used in some immunohistology experiments as controls for *plt/plt* mice that were backcrossed on the BALB/c background (BALB/c-*plt/plt*) (31). A newly constructed transgenic strain termed T-GFP (either FVB or crossed into C57/BL6/J background) served as the source of T^{GFP} cells (35). This study complies with NIH guidelines for the care and use of laboratory animals and was approved by the Institutional Review Committees of both Harvard Medical School and The Center for Blood Research. Mice were housed with free access to sterilized water and standard lab chow in a specific pathogen-free and viral antibody-free (SPF/VAF) animal facility at Harvard Medical School.

FACS® Analysis. Spleens and PLNs of T-GFP mice were passed through wire mesh in DMEM, 1% FCS, 20 mM Hepes, pH 7.4, containing 5 mM EDTA and depleted of erythrocytes by ammonium chloride lysis. After F_c receptors were blocked with anti-CD16/CD32, cells were stained with PE-conjugated anti-B220 or anti-CD3 mAb for 20 min on ice. Cells were washed and analyzed by flow cytometry (FACScan™; Becton Dickinson) using CELLQuest™ software (Becton Dickinson) after gating for viable lymphocytes by forward and side scatter characteristics.

Preparation of T-GFP Cells. To study selectively naive T cells in vivo, PLNs and MLNs of T-GFP mice were harvested, passed through wire mesh, and resuspended in 37°C DMEM, 1% FCS, 20 mM Hepes, pH 7.4. Naive T cells in T-GFP mice (henceforth called T^{GFP} cells) uniformly express high levels of GFP, whereas B cells and other leukocyte subsets do not (35; and this report). Single cell suspensions from T-GFP mice were injected into wild-type or *plt/plt* recipients without further purification or labeling. For intravital microscopy, lymphocytes were resuspended to 2×10^7 cells/ml in prewarmed buffer. For homing experiments, lymphocytes were resuspended to 2×10^8 cells/ml in DMEM, 1% FCS, 20 mM Hepes, pH 7.4. The behavior of T^{GFP} cells from animals on FVB or FVB × C57/BL6/J background was indistinguishable in intravital microscopy studies, homing experiments, and chemotaxis assays (not shown). Thus, data from both cell populations were pooled in Results (see below).

For desensitization, LN cells from T-GFP mice were prepared as above and incubated at 37°C for ≥40 min in DMEM, 1% FCS, 20 mM Hepes, pH 7.4, containing 1 μM SDF-1α or TCA-4. Desensitized cells were washed once, resuspended to 2×10^7 cells/ml, and immediately injected into recipients. Chemokine exposure did not affect GFP expression in T^{GFP} cells (not shown).

Immunohistology. Inguinal and axillary PLNs from wild-type and *plt/plt* mice were frozen in OCT compound (TBS). Serial sections (9 μm) were cut on a Leica cryostat, air dried, fixed in 2% paraformaldehyde, and incubated overnight at 4°C with anti-PNAd mAb MECA-79 (10 μg/ml) or a combination of anti–TCA-4 mAbs 4B1 and 3D5 (both at 200 μg/ml). These concentrations gave maximal signal while keeping background staining low. As a negative control for mAb MECA-79, rat serum (1:1,000) was used. After blocking intrinsic avidin/streptavidin, sections were incubated with biotinylated anti-Armenian hamster Ig (PharMingen) or anti–rat Ig (DAKO), then incubated with streptavidin–horseradish peroxidase (DAKO) followed by diaminobenzidine (DAB; Vector Laboratories) and counterstaining with hematoxylin.

Homing Assays. 5×10^7 T-GFP cells in 250 μl DMEM, 1% FCS, 20 mM Hepes, pH 7.4, were injected into the tail vein of age- and sex-matched DDD/1-*plt/plt* and DDD/1–*mtv-2/mtv-2* mice. After 2 h, mice were anesthetized and exsanguinated. Peripheral blood lymphocytes were isolated by ammonium chloride lysis of red

Downloaded from http://rupress.org/jem/article-pdf/191/1/61/1123529/99-0903.pdf by guest on 24 May 2022

blood cells. Recipient spleens, PLNs, MLNs, and PPs were dissected and passed through wire mesh. Single cell suspensions were analyzed by flow cytometry as described above. Data are expressed as percentage of GFP^+ cells in the total number of gated lymphocytes.

Animal Preparation. Mice were anesthetized by intraperitoneal injection of 10 ml/kg saline containing xylazine (1 mg/ml) and ketamine (5 mg/ml). The left subiliac (superficial inguinal) LN was prepared as described (10). In brief, the right femoral artery was catheterized for injection of cell samples and mAbs. Subsequently, a semicircular incision was made in the lower left abdominal skin. The skin flap was spread on a glass slide on a Plexiglas stage. The fatty tissue surrounding the exposed LN was removed without damage to feeding or draining blood vessels. In some experiments, 1 or 2.5 μg TCA-4 or SDF-1α in 50 μl Ringer's injection solution (Abbott Laboratories) was injected into the epidermis over the left thigh ~1 cm distally from the subiliac LN. Before preparing the LN, mice were allowed to rest for 30–45 min to maintain physiologic interstitial pressure gradients that may be necessary for chemokine-containing fluids to enter lymph vessels at the site of injection and for drainage into PLNs.

Distribution of Intracutaneously Injected ^{125}I–TCA-4. To assess the fate of intracutaneously injected TCA-4, 2.6 ng human ^{125}I–TCA-4 (96 mCi/mg) in 50 μl PBS was injected intracutaneously over the left anterior hind leg of BALB/c mice (three mice/time point). 15, 30, 60, 120, and 240 min after injection, mice were killed, the draining (left) and contralateral (right) subiliac LN and MLN were removed, and blood was obtained by cardiac puncture. Tissues were weighed, homogenized, agitated overnight on a shaker with 2 N NaOH and 0.05% SDS, and counted on a gamma-counter. The specific radioactivity associated with each organ was expressed per unit wet weight.

Measurement of TCA-4 by ELISA. Skin draining PLNs (axillary, cervical, and inguinal), MLNs, spleen, thymus, and PPs were harvested from young adult BALB/c or BALB/c-*plt/plt* mice. Some BALB/c-*plt/plt* mice were injected intracutaneously with 5 μg murine full-length TCA-4 or $TCA\text{-}4_{\Delta CT}$ that was equally distributed among five different injection sites (submandibular in the midline and bilaterally in ventral forelimbs and inner thighs; 50 μl PBS with 1 μg protein/site). The draining PLNs and other lymphoid organs were harvested 2 h later. 25 mg tissue was homogenized in 0.3 ml PBS with 1 mM PMSF, 0.01 mg/ml leupeptin, and 0.01 mg/ml aprotinin. Extracts were sonicated, centrifuged, and supernatants were stored at −80°C. TCA-4 in supernatants was detected by ELISA using immobilized mAb 4B1 for capture and biotinylated mAb 3D5 followed by alkaline phosphatase–coupled avidin (Pierce Chemical Co.) and 5 mM *p*-nitrophenyl phosphate (Sigma Chemical Co.) for detection. Both full-length TCA-4 and $TCA\text{-}4_{\Delta CT}$ can be quantified by this method with comparable sensitivity (not shown). Absorbency was determined at 405 nm with a Vmax® kinetic microplate reader (Molecular Devices). TCA-4 concentrations were calculated from standard curves obtained by titrating known amounts of TCA-4 or $TCA\text{-}4_{\Delta CT}$ into similar tissues from *plt/plt* mice.

Intravital Microscopy. Anesthetized animals were transferred to an intravital microscope (model IV-500; Mikron Instruments). Body temperature was maintained at 37°C using a tubular heater. LN microvessels were observed through a 40× water immersion objective (Achroplan, NA 0.75; Carl Zeiss, Inc.). For immunolocalization of TCA-4 in PLNs and skin, 75 μg FITC-conjugated mAb 4B1 in 250 μl saline was injected through the femoral artery catheter and allowed to bind for 5–30 min. In some animals, 75 μg FITC-conjugated anti-DNP mAb was injected as a nonbinding control.

Small boluses (20–50 μl) of LN cell suspensions from T-GFP mice were retrogradely injected through the femoral artery catheter and visualized in the subiliac LN by fluorescent epiillumination from a video-triggered xenon arc stroboscope (Chadwick-Helmuth) as described (10). This route of injection, directly upstream of the artery feeding the subiliac LN, allowed us to inject a second cell sample while keeping the systemic concentration of previously injected cells low (7). In some experiments, the role of LFA-1 in TCA-4–mediated sticking of T^{GFP} cells was assessed. After recording control T^{GFP} cell behavior without mAb, the recipient mouse and lymphocytes were treated with 50 μg (intra-arterial) and 20 μg/ml (5 min at 37°C) mAb TIB 213, respectively. Control and mAb-treated T^{GFP} cells were compared in the same vascular bed. At the end of each experiment, FITC-dextran (150 kD; 10 mg/kg) was injected to visualize the intravascular compartment for measurement of vascular dimensions (10). All scenes were recorded on videotape using a low-lag silicon-intensified target camera (model VE1000SIT; Dage MTI), a time base generator (For-A Corp. Ltd.), and a Sony Hi-8 VCR (model ECV-100).

Image Analysis. Video analysis was carried out off-line as described (36). Rolling (i.e., cells that interacted visibly with HEVs and traveled at a slower velocity than the blood stream) and noninteracting T^{GFP} cells were counted in each venule. The rolling fraction was calculated as percentage of rolling cells among the total number of T^{GFP} cells that entered a venule. The sticking fraction was determined as percentage of T^{GFP} cells becoming firmly adherent for >20 s in the number of T^{GFP} cells that rolled in a venule during the same time interval. Only venules in which ≥10 rolling cells were recorded were considered for analysis of sticking fractions. T^{GFP} cell adhesion was also analyzed in some HEVs with high blood flow that were located relatively deep within the LN. As the optical properties of these vessels were often suboptimal, it was not always possible to be certain that every fast moving noninteracting T^{GFP} cell could be detected. In contrast, rolling and sticking T^{GFP} cells produced a stronger signal in our camera and were reliably detected and quantified. Thus, only the sticking fraction was determined in these vessels. Lumenal cross-sectional diameters of FITC-dextran–filled vessels were measured using a customized image analysis system (37).

Statistical Analysis. Data are presented as mean ± SEM, unless otherwise indicated. For comparison of rolling and sticking fractions of different cell samples recorded in the same preparation, a paired Student's *t* test was used. For comparison of rolling and sticking fractions between different mouse preparations, the unpaired Student's *t* test was used. Significance was set at $P < 0.05$.

Online Supplemental Data. Digitized QuickTime™ videos showing characteristic scenes from intravital microscopy experiments of T^{GFP} cell behavior and TCA-4 staining in wild-type and *plt/plt* mice are available at http://www.jem.org/cgi/content/full/191/1/61/DC1 (see legends to Figs. 2, 4, 6, and 7).

Results

TCA-4 Protein Is Presented on the Luminal Surface of PLN HEVs in Wild-Type, but Not plt/plt Mice. This study was conducted to test the hypothesis that the chemokine TCA-4 mediates T cell homing to PLNs by activating LFA-1 on rolling T cells in HEVs. Our hypothesis was based on the recent finding that TCA-4 mRNA is expressed in PLN HEVs in wild-type mice (22), but not in *plt/plt* mice (33), which also have a striking defect in T cell homing to PLNs (31, 32). To

Downloaded from http://rupress.org/jem/article-pdf/191/1/61/1123529/99-0903.pdf by guest on 24 May 2022

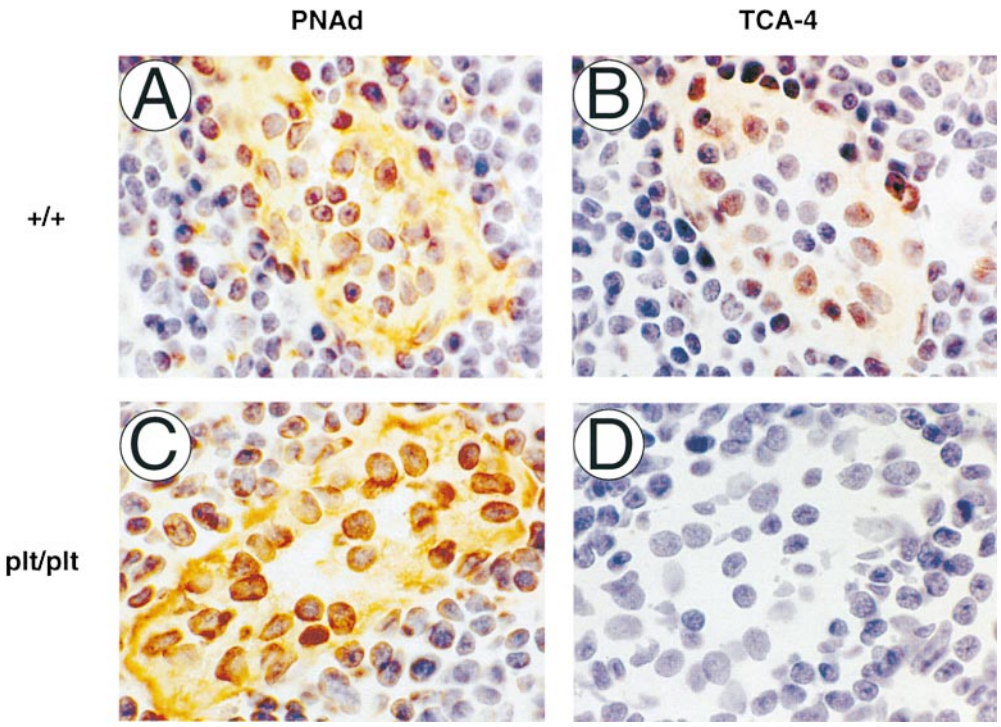

Figure 1. Expression of PNAd and TCA-4 in wild-type and *plt/plt* PLNs. Serial sections (9 μm) of wild-type (A and B) or *plt/plt* PLNs (C and D) were stained for PNAd (mAb MECA-79; A and C) or TCA-4 (mAbs 3D5 and 4B1; B and D). PNAd (A) and TCA-4 (B) are colocalized in wild-type HEVs. Although PNAd expression is normal in *plt/plt* HEVs (C), no TCA-4 can be detected in these animals (D). Original magnification: ×1,000.

determine whether the lack of TCA-4 message is reflected at the protein level, we performed immunohistology on serial LN sections from wild-type (DDD/1–*mtv-2/mtv-2* or BALB/c) and *plt/plt* mice. To identify HEVs, we used mAb MECA-79 against PNAd, an L-selectin ligand that stains PLN HEVs of all strains (31). Of 109 PNAd$^+$ HEVs that were identified in adjacent serial sections of wild-type PLNs ($n = 3$), 94 (86%) also stained with anti–TCA-4 (Fig. 1, A and B). In addition, single cells that were sparsely scattered throughout the T cell area stained weakly with anti–TCA-4. No staining was detected in B cell follicles (not shown). Although PNAd expression in *plt/plt* mice was comparable to wild-type mice (Fig. 1 C),

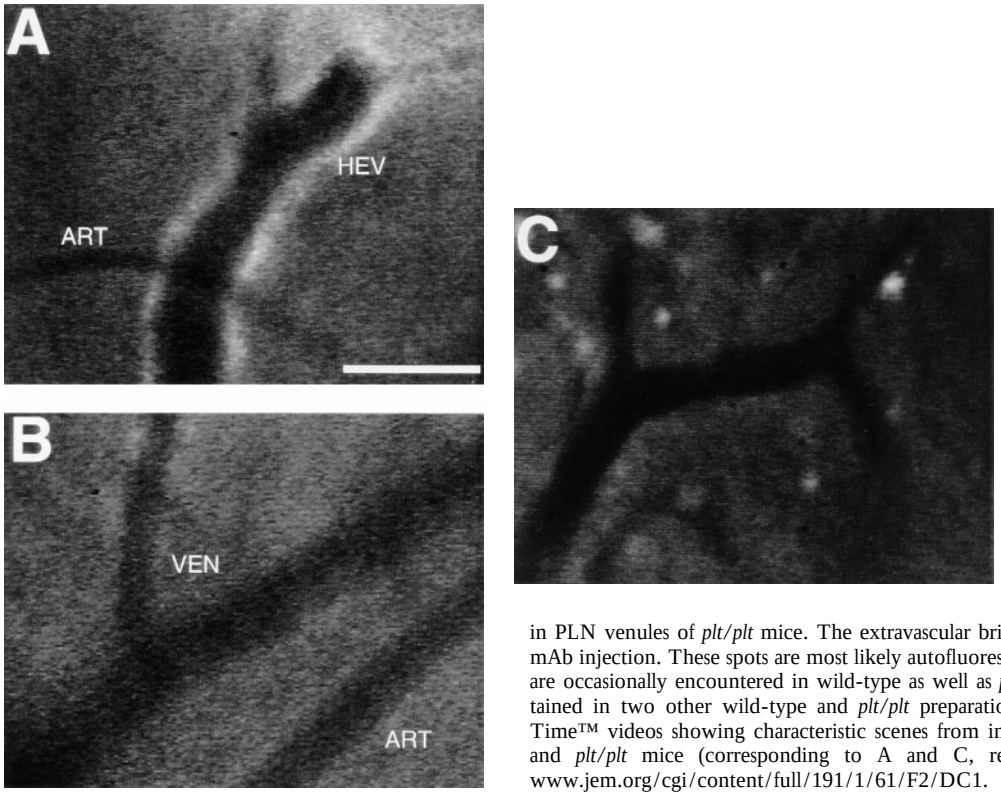

Figure 2. TCA-4 is presented on the luminal surface of wild-type, but not *plt/plt*, venules in PLNs. Fluorescent microvessels were recorded in anesthetized wild-type and *plt/plt* mice after intravenous injection of 75 μg anti–mouse TCA-4 mAb FITC-4B1. (A) PLN microvessels in a wild-type mouse. Note that fluorescent anti–TCA-4 delineates the HEV, but not an adjacent arteriole (ART). (B) Skin venules (VEN) or arterioles (ART) in the same wild-type mouse did not stain with anti–TCA-4. (C) FITC-4B1 did not accumulate in PLN venules of *plt/plt* mice. The extravascular bright spots were already present before mAb injection. These spots are most likely autofluorescent cells in the superficial cortex that are occasionally encountered in wild-type as well as *plt/plt* PLNs. Similar results were obtained in two other wild-type and *plt/plt* preparations. Bar, 100 μm. Digitized QuickTime™ videos showing characteristic scenes from intravital TCA-4 staining in wild-type and *plt/plt* mice (corresponding to A and C, respectively) are available at http://www.jem.org/cgi/content/full/191/1/61/F2/DC1.

Downloaded from http://rupress.org/jem/article-pdf/191/1/61/1123529/99-0903.pdf by guest on 24 May 2022

anti–TCA-4 did not bind detectably to HEVs or any other structure in *plt/plt* PLNs (Fig. 1 D).

The immunohistology technique used above does not have sufficient spatial resolution to distinguish between intracellular and surface-expressed antigen. We reasoned that HEV-associated TCA-4 in wild-type mice could only activate rolling T cells if it was presented on the luminal surface of HEVs. To address this issue in vivo, we injected FITC-conjugated anti–TCA-4 mAb 4B1 (75 μg intraarterial) into wild-type mice and observed the LN microvasculature by intravital microscopy as described (38). Within a few minutes after mAb injection, a striking accumulation of fluorescence was noted at the walls of most postcapillary and collecting venules, but not in arterioles or capillaries (Fig. 2 A). Maximum staining of PLN venules was observed after ~30 min, whereas no fluorescence was seen at any time point in the surrounding skin (Fig. 2 B). Consistent with the results obtained by immunohistology, no staining with anti–TCA-4 was observed anywhere within *plt/plt* LNs (Fig. 2 C). Injection of an equivalent amount of FITC-conjugated control mAb revealed no detectable staining in either mouse strain (not shown).

Use of T^{GFP} Cells for In Vivo Studies of T Cell Migration. Having confirmed that TCA-4 is expressed in HEVs of wild-type but not *plt/plt* PLNs, we asked whether this defect in *plt/plt* mice affects integrin activation on rolling lymphocytes. The *plt* mutation affects only T cell homing, whereas B cell migration is essentially normal (31, 32). Thus, it was necessary to study selectively T cell adhesion in PLN HEVs. For this purpose, we made use of transgenic T-GFP mice (35). The T-GFP transgene incorporates the promoter and proximal enhancer of murine CD4 (39) and pEGFP-C1 cDNA (Clontech), a red-shifted variant of wild-type GFP (P64L and S65T mutations), which is detectable by epifluorescence through an FITC filter set (35). The transcriptional control elements from the CD4 locus induced uniform GFP expression in essentially all naive $CD4^+$ and $CD8^+$ T cells (collectively called T^{GFP} cells). Other leukocyte subsets did not express the transgene (35; Fig. 3 A).

Experiments using flow cytometry and histology revealed no difference in size, cellularity, or composition of lymphoid organs in T-GFP mice compared with nontransgenic controls (35; and data not shown). To rigorously exclude that GFP expression in T^{GFP} cells had altered the cells' ability to home to PLNs, we performed short-term homing assays. 2 h after adoptive transfer, 6.0 ± 0.9% (mean ± SD; $n = 6$) of resident lymphocytes in PLNs of wild-type recipients were GFP^+ (Fig. 3 B), whereas T^{GFP} cells constituted only 1.3 ± 0.3% of lymphocytes in PLNs of *plt/plt* recipients ($n = 6$; $P < 0.0001$). On average, the total number of lymphocytes in wild-type PLNs is five times higher than in *plt/plt* PLNs (31; and data not shown). Thus, the absolute number of T^{GFP} cells that homed to PLNs was at least 20 times higher in wild-type than in *plt/plt* mice. In contrast, T^{GFP} homing to the spleen was similar in both strains (wild-type, 8.6 ± 1.8%; *plt/plt*, 7.7 ± 2.8%; $P = 0.31$). Conversely, the number of circulating T^{GFP} cells was larger in *plt/plt* than in wild-type mice (11.5 ± 3.2 vs. 2.6 ± 1.5%; $P < 0.0002$). These results are in good agreement with homing studies using

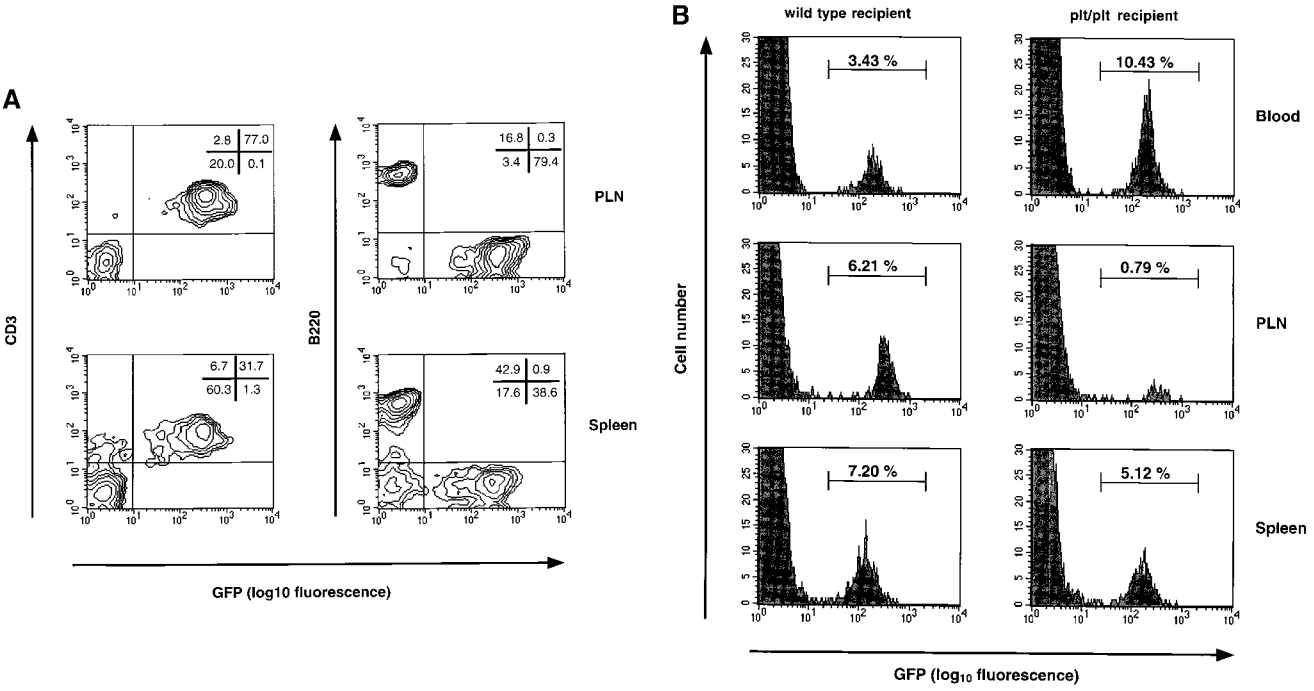

Figure 3. T lymphocytes from T-GFP transgenic mice specifically express GFP and serve as a useful tool for in vivo studies of T cell homing to PLNs. (A) FACS® analysis of splenocytes and PLN lymphocytes derived from T-GFP transgenic mice. Naive T, but not B cells from T-GFP transgenic mice specifically express GFP. (B) T^{GFP} homing to PLNs and spleen in wild-type and *plt/plt* mice. The distribution of T^{GFP} cells was analyzed 2 h after tail vein injection and expressed as percentage of GFP^+ cells among gated lymphocytes in each lymphoid organ and in systemic blood. One representative experiment (out of six performed with similar results) is shown for each recipient strain.

Downloaded from http://rupress.org/jem/article-pdf/191/1/61/1123529/99-0903.pdf by guest on 24 May 2022

nontransgenic T cells (31, 32) and indicate that T^{GFP} cells are useful for studying T cell migration.

T^{GFP} Cells Roll, but Do Not Arrest, in plt/plt HEVs. To analyze T cell behavior in PLNs, we generated single cell suspensions from PLNs and MLNs of T-GFP mice. Although these preparations contained only 60–80% T^{GFP} cells (Fig. 3 A), the cells were injected immediately into recipient mice without any further purification or labeling. Since T^{GFP} cells were the only subset carrying a fluorophore, contaminating nonfluorescent cells did not affect our analysis because they remained undetectable under epifluorescent light.

Consistent with the reduction in T cell numbers in *plt/plt* PLNs, the size of subiliac LNs appeared smaller and the venular tree had fewer branches than in wild-type controls (not shown). Moreover, most venules of the same branching order had a smaller diameter in *plt/plt* PLNs. For example, the diameter of order III venules in wild-type PLNs was 51.7 ± 6.2 μm (mean ± SEM; $n = 5$) vs. 25.1 ± 1.8 μm in *plt/plt* PLNs ($n = 9$; $P < 0.0003$). Consequently, the mean rolling fraction of T^{GFP} was somewhat higher in *plt/plt* PLNs (Fig. 4, A and B). It has been shown that rolling fractions tend to be inversely proportional to the vessel diameter, presumably because lymphocytes contact ECs more frequently in narrow vessels (10). No significant difference was found between wild-type and *plt/plt* LNs when rolling fractions were compared only in vessels of 25–40 μm diameter (44.2 ± 10.5%, $n = 5$, vs. 55.4 ± 4.1%, $n = 23$, respectively; $P = 0.27$).

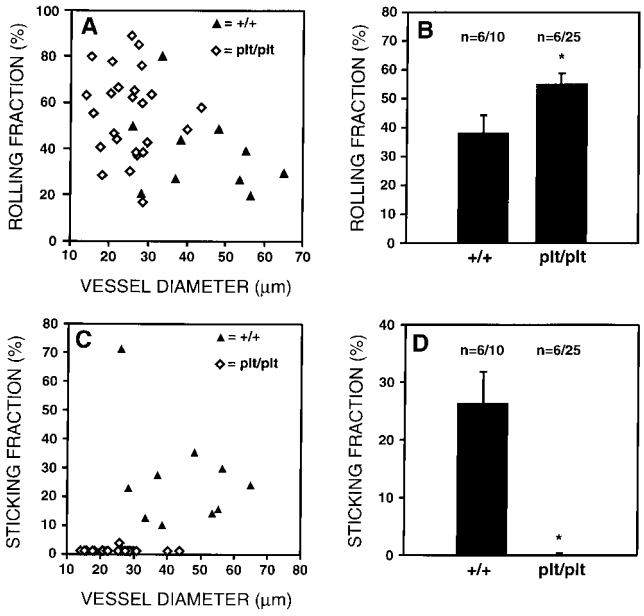

Figure 4. T^{GFP} cells roll in both wild-type and *plt/plt* PLNs, but only undergo firm adhesion in wild-type PLN venules. Using intravital microscopy of murine subiliac PLNs, the behavior of T^{GFP} cells was analyzed. (A) Rolling fractions (determined as the percentage of rolling cells in all cells passing through a given venule) of T^{GFP} cells in wild-type (+/+) and *plt/plt* PLN venules are shown as a function of vessel diameter. Each symbol represents a single venule. (B) Mean rolling fractions of T^{GFP} cells in wild-type and *plt/plt* HEVs. Rolling fractions are slightly elevated in *plt/plt* mice (*$P <$ 0.022). (C) Sticking fractions (percentage of rolling cells that arrest for at least 20 s) of T^{GFP} cells in wild-type and *plt/plt* PLN venules are shown as a function of vessel diameter. (D) Mean sticking fractions of T^{GFP} cells in wild-type and *plt/plt* PLN venules. Sticking is virtually absent in *plt/plt* PLN HEVs (*$P < 0.0001$). Data in B and D are shown as mean ± SEM; n = no. of animals/venules analyzed. Digitized QuickTime™ videos showing characteristic scenes from intravital microscopy experiments of T^{GFP} cell behavior in wild-type and *plt/plt* mice are available at http://www.jem.org/cgi/content/full/191/1/61/F4/DC1.

In wild-type mice, many rolling T^{GFP} cells adhered firmly (Fig. 4, C and D). The mean sticking fraction in order III and IV venules (21.4 ± 2.9%, $n = 5$, and 32.4 ± 14.2%, $n = 4$, respectively) was somewhat higher than previously published values derived from ex vivo–labeled LN cells of nontransgenic donors (7, 38; and our unpublished observations). In contrast, sticking was virtually absent in *plt/plt* HEVs. Only 1 cell in >700 rolling T^{GFP} cells analyzed remained stationary for ≥20 s, indicating that the transition from rolling to sticking is severely impaired in *plt/plt* mice.

Desensitization to TCA-4, but Not SDF-1α, Reduces T Cell Sticking in Wild-Type PLNs. Our findings in *plt/plt* mice pointed to a role for CCR7, the lymphocyte receptor for TCA-4, in LFA-1 activation on rolling T cells. To investigate whether the TCA-4/CCR7 pathway is similarly involved in T cell homing to wild-type PLNs, we took advantage of the observation that chemokine receptor responsiveness can be transiently blocked by prolonged exposure to an activating chemokine (24). T^{GFP} cells were exposed to either 1 μM TCA-4 or 1 μM SDF-1α (≥40 min at 37°C). The latter chemokine does not bind to CCR7, but it activates CXC chemokine receptor (CXCR)4, which is also expressed on naive T cells (40, 41). We injected first TCA-4–desensitized T^{GFP} cells and analyzed their behavior in PLNs within the first 15 min after desensitization. CCR7 remains refractory to TCA-4 signaling during this window of time (24). Subsequently, SDF-1α–desensitized T^{GFP} cells were recorded in the same preparation. The rolling fraction of both samples was similar and did not differ from untreated cells (Fig. 5 A), indicating that L-selectin function was not impaired by exposing cells to either chemokine. In contrast, T^{GFP} cells that

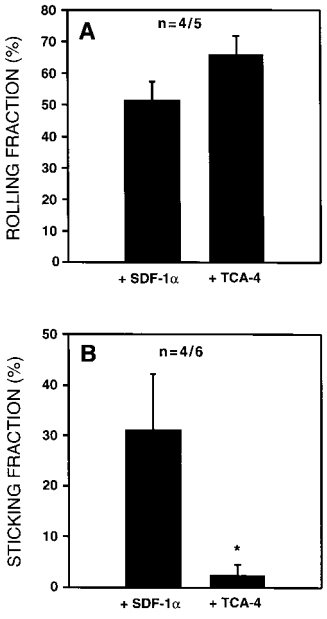

Figure 5. Desensitization of CCR7, but not CXCR4, in T^{GFP} cells blocks firm adhesion in wild-type PLN venules. T^{GFP} cells were desensitized by incubation for ≥40 min with 1 μM TCA-4 (agonist for CCR7) or 1 μm SDF-1α (agonist for CXCR4). Desensitized cells were sequentially injected into wild-type mice and observed in identical HEVs. (A) Mean rolling fractions of TCA-4– and SDF-1α–desensitized T^{GFP} cells. There was no statistically significant difference in rolling fractions. (B) Mean sticking fraction of TCA-4– and SDF-1α–desensitized T^{GFP} cells. T^{GFP} cells desensitized to TCA-4, but not SDF-1α, failed to undergo firm adhesion in wild-type PLN venules (*$P < 0.03$). Data are shown as mean ± SEM; n = no. of animals/venules analyzed.

Downloaded from http://rupress.org/jem/article-pdf/191/1/61/1123529/99-0903.pdf by guest on 24 May 2022

were refractory to TCA-4 arrested poorly in HEVs, whereas the sticking fraction of T^{GFP} cells desensitized to SDF-1α was not different from untreated controls (Fig. 5 B). Sticking fractions of SDF-1α–desensitized T^{GFP} cells were similar whether they were injected with or without prior injection of TCA-4–treated cells (data not shown). This indicates that the majority of T^{GFP} cells, which became stuck in PLNs of animals that had first received TCA-4–treated cells, were SDF-1α–desensitized T^{GFP} cells, and not rare recirculating TCA-4–desensitized cells from the prior injection.

Intracutaneously Injected TCA-4 Accumulates in Draining PLNs and Is Presented on HEVs. The concomitant lack of TCA-4 and T^{GFP} cell sticking in HEVs of *plt/plt* PLNs was consistent with the idea that TCA-4 is required for LFA-1 activation. However, these data did not constitute unequivocal proof for this concept, because it remained theoretically possible that the *plt* mutation affected other genes that may be required in addition to or instead of TCA-4. Therefore, we asked whether reconstitution of TCA-4 presentation in *plt/plt* HEVs could induce T^{GFP} cell sticking. Initially, we superfused surgically prepared subiliac LNs in *plt/plt* mice with a TCA-4–containing buffer. However, T^{GFP} cell sticking was not reproducibly induced by this approach (not shown). We reasoned that the fibrous capsule that covers the LN might have posed a diffusion barrier. Moreover, the surgical preparation necessary for microscopic viewing of the subiliac LN probably altered interstitial pressure gradients, and, thus, affected chemokine transport via lymph drainage. To test whether the chemokine could be transported via afferent lymph in animals that had not undergone surgery,

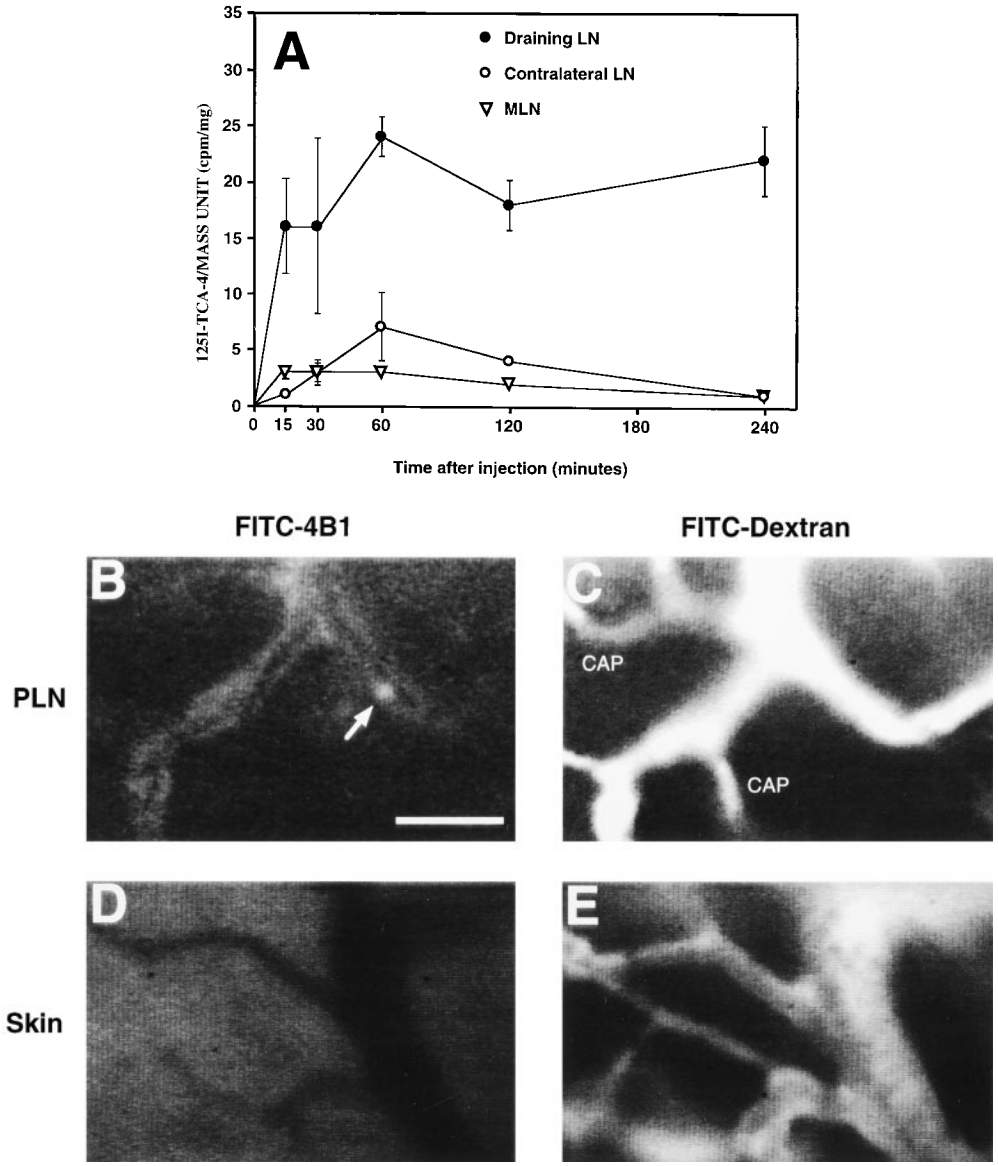

Figure 6. Intracutaneously injected TCA-4 specifically accumulates in draining PLNs, where it is presented on the luminal surface of HEVs. (A) ^{125}I–TCA-4 (2.6 ng in 50 μl saline) was injected into the skin over the left anterior hind leg of BALB/c mice, and radioactivity was determined at time points specified. The activity of ^{125}I–TCA-4 per mass unit organ was determined in draining (left) versus contralateral (right) subiliac LN and MLN as described in Materials and Methods. Three mice per time point after injection were analyzed. ^{125}I–TCA-4 specifically accumulated in the draining LN, whereas the contralateral LN and MLN remained largely unaffected. (B) Intravital micrograph of fluorescent anti–TCA-4 mAb FITC-4B1 staining (30 min after injection of the mAb) in a branched HEV of a draining subiliac LN of a *plt/plt* mouse 2 h after intracutaneous injection of TCA-4. 2.5 μg TCA-4 was injected intracutaneously in the left hind leg, and the draining subiliac LN was observed after intraarterial injection of 75 μg anti–TCA-4 mAb FITC-4B1. FITC-4B1 accumulated in some, but not all PLN microvessels. Note that the right venular branch is only partially labeled, and capillaries are not stained at all (see C). An interacting T^{GFP} cell can be seen in the right venular branch (arrow). A digitized QuickTime™ video of this scene is available at http://www.jem.org/cgi/content/full/191/1/61/F6/DC1. (C) Micrograph of the same field of view as in B after injection of FITC-dextran (150 kD) as a plasma marker. Note that FITC-dextran, unlike anti–TCA-4 mAb, delineates all capillaries (CAP) and venules, including the entire length of the HEV that enters the field of view from the right margin. (D) A skin venule in the same preparation 2 h after intracutaneous injection of TCA-4 and 30 min after injection of anti–TCA-4 mAb FITC-4B1. No specific fluorescence is associated with these nonlymphoid vessels. (E) Micrograph of the same field of view as in D after injection of FITC-dextran. Bar, 50 μm.

Downloaded from http://rupress.org/jem/article-pdf/191/1/61/1123529/99-0903.pdf by guest on 24 May 2022

we injected ^{125}I–TCA-4 into the skin over the left thigh of BALB/c mice. ^{125}I–TCA-4 accumulated in the draining (left) subiliac LN, but not in the contralateral (right) node or in MLNs (Fig. 6 A). A signal was detected in draining LNs as early as 15 min after injection. At 4 h, the draining node contained 20 times more ^{125}I–TCA-4 than the contralateral node and 10 times more than the peripheral blood (not shown). High levels of ^{125}I–TCA-4 were also observed in the kidney (not shown). This probably reflects the route of chemokine clearance, as has been shown for IL-8 (Rot, A., unpublished data).

To estimate the amount of intracutaneously injected TCA-4 that reaches *plt/plt* PLNs, TCA-4 was injected into the skin over the neck and bilaterally in the ventral forelimbs and inner thighs of BALB/c-*plt/plt* mice. 2 h later, the TCA-4 concentration in lymphoid organs was determined by ELISA (Table I). TCA-4 levels in untreated BALB/c-*plt/plt* mice were below the detection limit (0.01 ng/mg tissue) of our assay. In contrast, significant levels of TCA-4 (~20% of wild-type) were achieved in skin draining PLNs of BALB/c-*plt/plt* mice that had received TCA-4 intracutaneously. TCA-4 was undetectable in most other lymphoid organs, except the spleen. Interestingly, TCA-$4_{\Delta CT}$ lacking 41 amino acids of the elongated COOH terminus accumulated less in draining LNs or other lymphoid tissues when an equivalent amount was injected (Table I).

Next, we asked whether intracutaneously injected exogenous TCA-4 in draining PLNs can be transported to and presented within HEVs. We injected 2.5 μg TCA-4 into the skin over the subiliac LN of *plt/plt* mice. 30 min later, the LN was prepared for intravital microscopy. 90–120 min after chemokine injection, anti–TCA-4 mAb FITC-4B1 was administered intraarterially. In contrast to untreated *plt/plt* mice (Fig. 2 C), several venules in draining PLNs of TCA-4–treated *plt/plt* mice acquired a faint but detectable fluorescent signal (Fig. 6 B). No fluorescence was seen in LN capillaries or arterioles or in skin microvessels (Fig. 6, C–E). Interestingly, anti–TCA-4 delineated some, but not all venules in *plt/plt* PLNs, and a few venules were observed in which staining appeared to be segmental. These findings suggest that intracutaneously injected exogenous TCA-4 not only reaches PLNs via afferent lymph, but is also transported to the luminal surface of some PLN HEVs.

Intracutaneously Injected TCA-4 Reconstitutes LFA-1–mediated Sticking of T^{GFP} Cells in plt/plt HEVs. We investigated the effect of exogenous TCA-4 on T^{GFP} cell adhesion. For this, *plt/plt* animals received intracutaneous injections of either 1 μg TCA-4 or 1 μg SDF-1α in 50 μl Ringer's injection solution. 30 min later, the draining subiliac LN was prepared for intravital microscopy, and T^{GFP} cell behavior in HEVs was recorded 60–90 min thereafter. Rolling fractions remained unchanged compared with untreated *plt/plt* mice (Fig. 7, A and B). In contrast, in each of eight PLNs of TCA-4–treated mice, HEVs were detected that supported significant sticking of T^{GFP} cells (Fig. 7 D). Overall, sticking was observed in 13 out of 34 recorded *plt/plt* HEVs, with a maximum sticking fraction of 36.7%, a value that was comparable to sticking fractions in wild-type HEVs (Fig. 4 C) but was never observed in untreated *plt/plt* mice (Fig. 7 C). In contrast, intracutaneous injection of SDF-1α did not induce T cell arrest, except in one *plt/plt* mouse (out of five) in which two HEVs supported some sticking (Fig. 7, E and F).

To determine whether the effect of intracutaneously injected TCA-4 on T^{GFP} cells was due to LFA-1 activation, HEVs in TCA-4–treated *plt/plt* animals were identified that supported significant sticking of T^{GFP} cells. Subsequently, the mice and cells were treated with anti–LFA-1, and T^{GFP} cell sticking was compared in the same venules. Inhibition of LFA-1 nearly abrogated TCA-4–induced T^{GFP} cell sticking in all vessels (Fig. 8).

Discussion

Previous work has shown that lymphocyte homing to PLNs is mediated by a multistep adhesion and signaling cas-

Table I. *TCA-4 Concentration in Lymphoid Organs of BALB/c and BALB/c-plt/plt Mice with or without Intracutaneous Injection of TCA-4 or TCA-$4_{\Delta CT}$*

Tissue	Recoverable TCA-4 (ng/mg wet wt)			
	BALB/c	BALB/c-*plt/plt*	BALB/c-*plt/plt* + TCA-4 i.c.	BALB/c-*plt/plt* + TCA-$4_{\Delta CT}$ i.c.
PLN	2.56 ± 0.37	<0.01	0.54 ± 0.32	0.04 ± 0.01
MLN	4.37 ± 1.86	<0.01	<0.01	<0.01
PP	1.87 ± 0.50	<0.01	<0.01	<0.01
Thymus	0.78 ± 0.25	<0.01	<0.01	<0.01
Spleen	0.20 ± 0.14	<0.01	0.18 ± 0.07	0.03 ± 0.01

Chemokine concentrations in homogenized lymphoid tissues were measured by capture ELISA. Some BALB/c-*plt/plt* mice received intracutaneous (i.c.) injections of a total of 5 μg recombinant murine full-length or truncated TCA-4 distributed to five anatomical sites as described in Materials and Methods. Tissues were harvested 2 h later, at which time full-length TCA-4 was detectable in draining PLNs (axillary, cervical, and inguinal LNs) and the spleen, but not in other lymphoid tissues. On the other hand, TCA-$4_{\Delta CT}$ failed to accumulate in draining LNs and other lymphoid tissues. Results are shown as mean ± SEM from four to eight mice per group.

Downloaded from http://rupress.org/jem/article-pdf/191/1/61/1123529/99-0903.pdf by guest on 24 May 2022

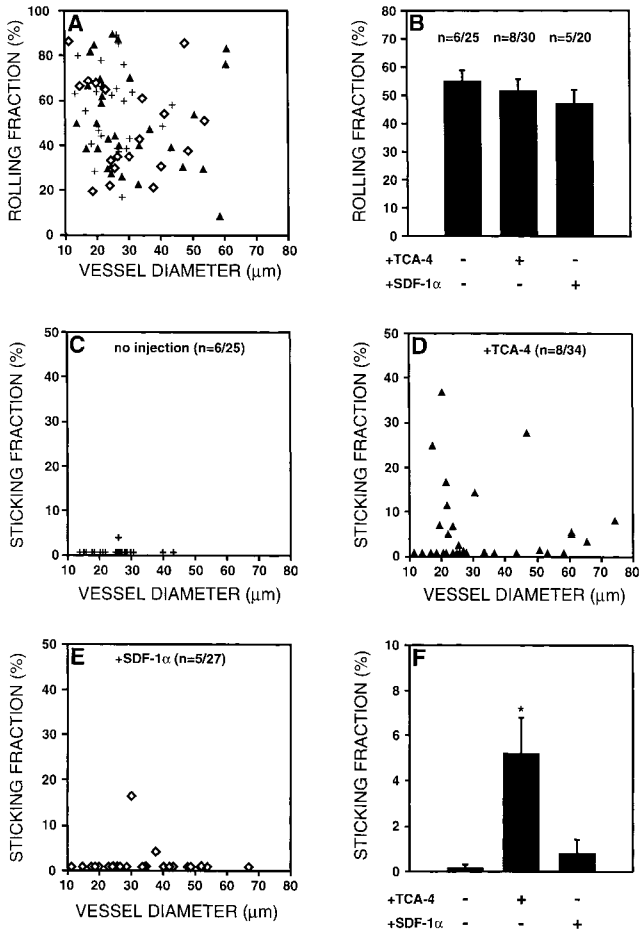

Figure 7. Intracutaneously injected TCA-4, but not SDF-1α, reconstitutes T^{GFP} cell sticking in *plt/plt* PLN venules. 1 μg TCA-4 or SDF-1α was injected intracutaneously in left hind legs of *plt/plt* mice. Surgical preparation of the draining left inguinal LN was started 30–40 min after chemokine injection. T^{GFP} cell behavior was observed in the draining subiliac PLN 90 min after chemokine injection using intravital microscopy. (A) Rolling fractions of T^{GFP} cells in *plt/plt* PLN venules without chemokine injection (+) or after injection of 1 μg TCA-4 (▲) or SDF-1α (◇) as a function of vessel diameter. (B) Mean rolling fractions of T^{GFP} cells in *plt/plt* PLN venules. The rolling frequency was not affected by chemokines. (C–E) Sticking fractions of T^{GFP} cells in *plt/plt* PLN venules without chemokine injection (C) or after pretreatment with TCA-4 (D) or SDF-1α (E) as a function of the vessel diameter. (F) Mean sticking fractions of T^{GFP} cells in *plt/plt* PLN venules. T^{GFP} cells underwent firm adhesion in some, but not all, HEVs of TCA-4–pretreated *plt/plt* mice (*$P < 0.008$ vs. no chemokine, and $P < 0.02$ vs. SDF-1α–treated animals). On the other hand, SDF-1α–pretreated *plt/plt* PLN venules did not support firm adhesion of T^{GFP} cells, except in one animal (out of five) where some sticking was seen in two venules ($P = 0.34$ vs. no chemokine). Data are shown as mean ± SEM; n = no. of animals/venules analyzed. A digitized QuickTime™ video showing T cell rolling and sticking in an HEV of a plt/plt mouse 1 h after intracutaneous injection of TCA-4 is available at http://www.jem.org/cgi/content/full/191/1/61/F7/DC1.

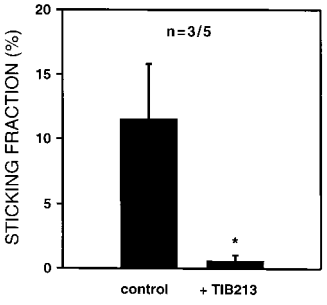

Figure 8. TCA-4–induced firm arrest of T^{GFP} cells in *plt/plt* HEVs is LFA-1 dependent. Mean sticking fractions of T^{GFP} cells in *plt/plt* HEVs pretreated with TCA-4 before and after anti–LFA-1 mAb (TIB 213) treatment. After assessment of T^{GFP} cell sticking in the absence of mAb (control), mice and GFP-T cells were treated with anti–LFA-1 mAb and observed in the same HEVs that supported firm arrest of control cells. In contrast to untreated T^{GFP} cells, anti–LFA-1 mAb–treated T^{GFP} cells failed to become firmly adherent (*$P < 0.05$). Data are shown as mean ± SEM; n = no. of animals/venules analyzed.

cade (7). Upon entry into HEVs, L-selectin tethers fast moving cells to PNAd on the endothelial lining. The L-selectin/PNAd pathway mediates rolling whether the tethered cells are PLN-homing lymphocytes or leukocytes (e.g., granulocytes) that do not accumulate in normal PLNs (7). The selectivity of lymphocyte recruitment to PLNs has been attributed to the fact that lymphocytes are the predominant rolling population that can arrest in HEVs. Sticking requires LFA-1, which is found on all leukocytes, but it must be functionally activated to bind to endothelium. LFA-1 activation in HEVs is known to depend on $G\alpha_i$ protein signaling (7, 17, 42). Since neither the primary (L-selectin) nor the secondary (LFA-1) adhesion receptors are uniquely expressed on PLN-homing (predominantly naive) lymphocytes, it has been proposed that the integrin-activating stimulus, which has been unknown, is critical for the overall specificity of the adhesion cascade.

Here, we report that constitutively expressed TCA-4 in PLN HEVs provides a subset-specific signal to rolling T cells that triggers rapid LFA-1 activation. Several lines of evidence suggest that TCA-4 is both necessary and sufficient to induce LFA-1–dependent arrest of T cells in PLN HEVs. First, using immunofluorescence microscopy in live animals, we found that TCA-4 was presented on the luminal surface of HEVs. Second, TCA-4–desensitized T cells failed to stick in wild-type PLNs. Third, PLN HEVs in *plt/plt* mice did not express TCA-4 and did not support T cell sticking, resulting in markedly reduced T cell homing to PLNs. Finally and most importantly, LFA-1–mediated T cell arrest was restored in *plt/plt* PLNs whose HEVs presented intracutaneously injected exogenous TCA-4. It has been postulated for some time that chemokines serve as selective triggers of integrin activation during lymphocyte homing (2, 3, 18, 19). To our knowledge, this is the first study to provide direct evidence for this concept in vivo.

Our results are consistent with earlier observations that have led to the speculation that TCA-4 is involved in T cell homing to PLNs (22, 24, 28, 29, 43). One of the first clues was the finding that TCA-4 mRNA is constitutively expressed in HEVs (22). Further, the predominant receptor for TCA-4 is CCR7, a $G\alpha_i$-linked serpentine glycoprotein on PLN-tropic T and B cells, not found on granulocytes or monocytes (24, 25). In vitro, not only is TCA-4 a potent chemoattractant for B and T cells in assays that last a few hours (20–24, 43), but it can also induce integrin-mediated adhesion within seconds (28–30). This is important, considering the short transit time of lymphocytes through PLN HEVs (7, 10). Finally, it was shown recently that HEVs in

Downloaded from http://rupress.org/jem/article-pdf/191/1/61/1123529/99-0903.pdf by guest on 24 May 2022

plt/plt mice do not contain TCA-4 message (33). Previous work has demonstrated that T cells home poorly to PLNs of *plt/plt* mice, whereas B cell homing is normal. This phenotype was due to an autosomal recessive defect affecting the PLN stroma (31, 32).

Since these earlier findings were suggestive of a role for TCA-4 during homing of T cells, but not B cells, to PLNs, we undertook this study. We used a novel strategy to visualize selectively T cells by intravital fluorescence microscopy. In previous studies, lymphocyte subpopulations were isolated and fluorescently labeled to detect adoptively transferred cells in recipient animals (7, 38, 42, 44). Such manipulations might alter the function of isolated cells. For example, we observed that exposure of adoptively transferred LN cells to cold temperature or culture for several hours before injection often reduced the cells' ability to stick in PLN HEVs (7; and our unpublished data). Such confounding factors are difficult to avoid when a large number of homogenous cells must be obtained by conventional isolation methods. Furthermore, contaminating cell populations can potentially alter the experimental readout. To circumvent these problems, we used T-GFP mice in which transgenic GFP is selectively expressed in $CD4^+$ and $CD8^+$ T cells (35). Most effector and some memory T cells in these animals lose GFP expression, whereas cells that express GFP at detectable levels are naive T cells (35). Single cell suspensions were generated from LNs of T-GFP donors and injected into recipients within 1 h after harvesting. Any transferred non-T cells (as well as the recipients' own leukocytes) remained invisible when viewed under epifluorescent light.

To ensure that transgenic GFP did not alter T cell behavior, we performed short-term homing assays and intravital microscopy. Consistent with previous studies on nontransgenic T cells (31, 32), T^{GFP} cells homed to wild-type PLNs, but migrated poorly to *plt/plt* PLNs. T^{GFP} cells expressed physiological levels of L-selectin (35), and their rolling fraction in PLN HEVs was comparable to that of nontransgenic lymphocytes (7, 38), indicating that L-selectin function was normal. Interestingly, sticking fractions of T^{GFP} cells in wild-type PLN HEVs tended to be higher than those observed previously with ex vivo–labeled nontransgenic LN cells (7, 38). This may have had two reasons. First, the LN cells used in earlier studies contained ~30% B cells, which home at a lower frequency to PLNs than T cells (45). Although B cells have not been specifically examined in the PLN model, it is possible that their sticking fraction is lower, which may have had a diluting effect on the overall sticking frequency of mixed LN cells. Second, as discussed above, T^{GFP} cells require only minimal manipulation, whereas nontransgenic lymphocytes must be subjected to procedures that might reduce their ability to engage integrins. The increased capacity of T^{GFP} cells to activate LFA-1 might thus reflect a more physiological phenotype.

To test T^{GFP} cell responsiveness to TCA-4, we performed chemotaxis assays across polycarbonate filter membranes (46). T^{GFP} cells and nontransgenic T cells migrated avidly and with equivalent frequency toward a TCA-4 gradient. This response was mediated by TCA-4 binding to CCR7, because TCA-4–induced T cell migration was abolished when macrophage inflammatory protein (MIP)-3β, another CCR7 agonist (47), was added to the top chamber (not shown). TCA-4 can also bind to murine CXCR3, a chemokine receptor that is reportedly expressed on activated Th1 cells, but not on naive T cells (48). However, the CXCR3 agonist monokine induced by IFN-γ (MIG), did not attract T^{GFP} cells and did not antagonize TCA-4–induced T^{GFP} cell migration. Thus, CCR7, and not CXCR3, was the principal TCA-4 receptor on T^{GFP} cells (not shown).

Having determined that T^{GFP} cells are useful to study the role of the TCA-4/CCR7 pathway in T cell homing, we initially treated wild-type mice with anti–TCA-4 mAbs 3D5 and 4B1. Both mAbs block T^{GFP} cell chemotaxis toward TCA-4 in vitro (20; and data not shown). However, the mAbs did not affect T^{GFP} cell adhesion or homing to PLNs, even when given at high doses, either alone or in combination. When anti–TCA-4 mAbs were added at a concentration that inhibited chemotaxis to L1-2 transfectants expressing murine CCR7, neither blocked TCA-4–induced intracellular calcium flux (not shown). Thus, the mAbs did not antagonize TCA-4 binding to or signaling through CCR7. The mechanism by which they inhibit chemotaxis is unclear. In any case, our findings indicate that blocking activities of antibodies against chemokines in chemotaxis assays must be interpreted with caution. Furthermore, since anti–TCA-4 mAbs did not block TCA-4 signaling via CCR7, the lack of a detectable effect in vivo does not argue against a role for this pathway in T cell homing.

Therefore, we explored alternative strategies to address this question. One approach was to examine the effect of TCA-4 desensitization. T^{GFP} cells were incubated with TCA-4 or SDF-1α under conditions that render their respective receptors, CCR7 and CXCR4, transiently unresponsive, whereas other chemokine receptors remain functional (24). Although SDF-1α, a ubiquitously expressed chemokine, can activate lymphocyte LFA-1 under flow (28), CXCR4-deficient lymphocytes home efficiently to secondary lymphoid organs (49). As SDF-1α is thus apparently not essential for homing to PLNs, we chose it to control for nonspecific effects that might occur during desensitization. A recent study reported that lymphocyte desensitization to SDF-1α inhibits calcium signaling in response to CCR7 stimulation by MIP-3β (50). However, when we examined L1-2 cells that expressed CXCR4 and stably transfected murine CCR7, we found no cross-desensitization between SDF-1α and TCA-4 in calcium flux assays (not shown). Moreover, SDF-1α did not interfere with T cell chemotaxis toward TCA-4 (24; and our unpublished data). Thus, desensitization to SDF-1α did not affect the T cell response to TCA-4 and vice versa. When desensitized T^{GFP} cells were tested in vivo, rolling was not altered, but TCA-4–desensitized T^{GFP} cells failed to stick in HEVs. Similarly, when CCR7 was desensitized to MIP-3β, sticking of T^{GFP} cells was abolished (not shown), indicating that CCR7, but not CXCR4, is required for T cell arrest in PLN HEVs. This

Downloaded from http://rupress.org/jem/article-pdf/191/1/61/1123529/99-0903.pdf by guest on 24 May 2022

cannot be explained by differential expression or signaling of the two receptors, because both are expressed on naive T cells (24, 51) and both can induce rapid integrin activation in vitro (28).

The most likely explanation for these results is that PLN HEVs contain agonists that stimulate CCR7, but not CXCR4, on rolling T cells. Indeed, wild-type PLN HEVs rapidly accumulated circulating fluorescent anti–TCA-4, indicating that TCA-4 is presented on the luminal surface of these vessels. The mAb did not delineate arterioles, or capillaries in PLNs, nor did it stain adjacent skin venules. Thus, TCA-4 presentation is a specialized feature of HEVs analogous to the expression of PNAd, which shows a similarly restricted distribution in vivo (38). The fluorescent mAb was apparently retained in HEVs, suggesting that its antigen was somehow immobilized, even though TCA-4 is a secreted molecule and has no transmembrane domain (20–23). However, like most chemokines, TCA-4 contains COOH-terminal binding sites for heparin-like glycosaminoglycans (GAGs) (20–23). Since sulfated glycosaminoglycans are highly concentrated in HEVs (52), it is conceivable that TCA-4 is retained and presented by such molecules. This is consistent with the concept that integrin-activating factors must be presented to rolling leukocytes in a manner that keeps them from being dispersed by the flowing blood (53–55). This notion was underscored by recent experiments with full-length and COOH-terminally truncated IL-8 in rabbits (53). Both activated neutrophils equally well in vitro, but only the former was presented on the luminal surface of ECs and promoted neutrophil accumulation upon intracutaneous injection, whereas the latter did not (53).

Although our findings with desensitized T cells are consistent with a role for CCR7 in T cell sticking in HEVs, they cannot distinguish between different CCR7 agonists (i.e., TCA-4 versus MIP-3β). Also, we cannot rule out that prolonged exposure to TCA-4 affected the T^{GFP} cells' response to other chemoattractants. Therefore, we performed experiments in *plt/plt* mice. In situ hybridization has shown that TCA-4 mRNA is absent in *plt/plt* PLN HEVs (33). Using immunohistochemistry and in vivo labeling with fluorescent anti–TCA-4, we show that TCA-4 protein is also undetectable. Homing assays with T^{GFP} cells further confirmed the severe defect in T cell recruitment to PLNs (31, 32). A few T^{GFP} cells were still found in *plt/plt* PLNs. Some of these cells may have been localized in blood that could not be completely removed from the harvested PLNs. Adding to this background, the percentage of T^{GFP} cells in *plt/plt* blood was significantly higher than in wild-type mice, probably resulting from the inability of T^{GFP} cells to leave the vascular compartment in *plt/plt* animals (31). However, *plt/plt* PLNs are not entirely devoid of lymphocytes, but contain essentially normal numbers of B cells and some T cells that are predominantly of memory phenotype (32). Thus, alternative mechanisms exist in PLNs that mediate homing of B cells and possibly also of distinct (memory) T cell subsets in the absence of TCA-4.

Nevertheless, our intravital microscopy studies clearly show that naive T cells are incapable of arresting in *plt/plt* HEVs, indicating that the *plt* phenotype is due to a defect in the transition from L-selectin–mediated rolling to integrin-dependent sticking. However, although TCA-4 is clearly not expressed in *plt/plt* PLNs, it cannot be excluded that the *plt* mutation also affects other relevant loci besides TCA-4. For example, the MIP-3β gene lies within 100 kb of the TCA-4 locus, and MIP-3β mRNA is also somewhat reduced in *plt/plt* PLNs (33). In contrast to TCA-4, MIP-3β is not expressed by HEVs, but by interdigitating DCs (27) whose migration to the T cell area of *plt/plt* PLNs is compromised (33). While this DC migration defect (which may be related to the absence of TCA-4) could explain the reduction in MIP-3β message, this circumstance complicates the interpretation of our results. If MIP-3β protein is similarly reduced (this is presently unknown), the lack of this CCR7 agonist (and/or other DC-derived mediators) could provide an alternative explanation for the absence of T cell sticking in *plt/plt* PLNs.

To obtain direct proof that TCA-4 deficiency is at least in part responsible for the lack of T cell sticking in *plt/plt* HEVs, we set out to reconstitute TCA-4 presentation in these vessels. This was possible because intracutaneously injected recombinant full-length, but not COOH-terminally truncated, TCA-4 accumulated rapidly in draining LNs and was transported to the lumen of some HEVs. Indeed, intracutaneously injected exogenous TCA-4 reconstituted LFA-1–dependent sticking of T^{GFP} cells in *plt/plt* PLNs. Although sticking was limited to only about one third of the observed HEVs, it was significantly higher than in untreated or SDF-1α–treated *plt/plt* mice. Injection of SDF-1α into the skin of mice has been shown previously to cause a local inflammatory response (51), but it did not alter T^{GFP} cell behavior in draining PLNs. Therefore, it seems likely that T^{GFP} cell sticking in *plt/plt* PLNs was a direct result of TCA-4 presentation in HEVs, rather than secondary inflammation-induced events that might be elicited by intracutaneous injection of chemokines.

An interesting question is how TCA-4 was transported from the skin to the luminal surface of PLN HEVs. The rapidity and selectivity at which intracutaneously injected TCA-4 appeared in PLNs that drained the site of injection indicate that its primary access route was afferent lymph vessels. Of note, it has been shown that some CC chemokines bind to dermal lymph vessels, suggesting that lymphatic ECs can control the uptake (and possibly drainage) of certain chemokines (56). It is unknown whether the transport of TCA-4 or SDF-1α is regulated at this level. The finding that intracutaneously injected $TCA\text{-}4_{\Delta CT}$ was barely detectable in draining PLNs suggests that the elongated COOH terminus of TCA-4 could be involved. This unexpected observation suggests the existence of specific molecular recognition and transportation mechanisms and indicates that the drainage of TCA-4 (and perhaps other chemokines) to PLNs cannot be explained by mere passive diffusion and lymph flow along hydrostatic pressure gradients.

Once TCA-4 has reached the PLNs, it is apparently transported to HEVs. One candidate intranodal pathway may be the fibroblastic reticular cell conduit system, a mesh-

Downloaded from http://rupress.org/jem/article-pdf/191/1/61/1123529/99-0903.pdf by guest on 24 May 2022

work of fiber-like channels that drains afferent lymph fluid from the subcapsular sinus to the vicinity of HEVs (57, 58). In addition, some intracutaneously injected TCA-4 can apparently reach the blood either directly or possibly via lymph drainage through the thoracic duct. This could explain the appearance of TCA-4 in the spleen of *plt/plt* mice 2 h after intracutaneous injection. Thus, it cannot be excluded that blood-borne TCA-4 can also bind to HEVs and contribute to the reconstitution of sticking. However, intracutaneously injected TCA-4 accumulated preferentially in draining PLNs where only a subset of HEVs was stained with anti–TCA-4 mAb and supported sticking of T^{GFP} cells. This argues against a significant contribution by blood-borne TCA-4, which should be more evenly distributed. Rather, this pattern probably reflects restricted drainage or transport of lymph fluid within the node.

Transport of abluminal TCA-4 to the luminal surface of HEVs might be achieved by diffusion between adjacent ECs (57, 58) or, perhaps more likely, by specific transendothelial movement. Endocytotic uptake, transcytosis, and presentation of chemokines on microvillus-like luminal surface protrusions were described for IL-8 and regulated upon activation, normal T cell expressed and secreted (RANTES) in skin microvessels (53). Conceivably, the unusually long, basic COOH terminus of TCA-4 may play a role not only in transportation from the skin to PLNs, but also in its translocation to the luminal surface of HEVs, possibly in conjunction with specialized proteoglycans. A role for chemokine association with proteoglycans in intracellular vesicles has been reported in cytolytic T cells (59). In addition, the COOH terminus might help to retain TCA-4 on the luminal surface of HEVs complexed to proteoglycans. Accordingly, preliminary experiments suggest that the COOH terminus increases retention of TCA-4 on heparan sulfate (Luo, Y., unpublished observations).

Since TCA-4 is constitutively synthesized by HEVs, it is unclear whether its transport via afferent lymph or its translocation across the venular wall plays a physiological role in lymphocyte homing to PLNs. However, it seems likely that other molecules can share this conduit. For example, PLN venules require afferent lymph fluid to maintain an HEV phenotype (60–62). Furthermore, recent findings indicate that mast cell–derived MIP-1β can be transported to and presented within HEVs in inflamed PLNs (63). MIP-1β has also been detected in the fibroblastic reticular cell conduit system (58). We speculate that transportation of specialized chemokines via afferent lymph constitutes a "remote control" mechanism that modulates the composition of leukocyte subsets that are recruited to PLNs.

In conclusion, we report that TCA-4 is presented on the luminal surface of PLN HEVs where it interacts with CCR7 on rolling T cells to activate LFA-1–mediated arrest. In this study, we exploited the fact that adoptively transferred naive T cells from transgenic T-GFP mice can be readily identified in PLN HEVs. Desensitization of T^{GFP} cells to TCA-4 abolished LFA-1–dependent sticking in wild-type HEVs, and untreated T^{GFP} cells did not stick in PLN HEVs of *plt/plt* mutant mice, which have a genetic defect in TCA-4 expression. Indeed, after this paper was accepted for publication, a report by Vassileva et al. (64) demonstrated the presence of two TCA-4 genes in mice. Only one of these genes is expressed in lymphoid tissues. Consistent with the data presented here, it was shown that this gene is deleted in *plt/plt* mice, whereas the other (responsible for TCA-4 expression in some nonlymphoid tissues) remains intact. TCA-4 presentation, as well as T^{GFP} cell sticking, in *plt/plt* PLN HEVs was restored by intracutaneous injection of TCA-4. Although these results do not exclude a contribution by other chemoattractants to T cell homing to PLNs, our data suggest that TCA-4 is both necessary and sufficient to activate integrins on rolling T cells in HEVs. Since T cell homing to MLNs and PPs is also compromised in *plt/plt* mice (32; and data not shown), we propose that TCA-4 may have a similar role in most secondary lymphoid tissues, except the spleen.

We also demonstrate that chemokines can be transported over long distances to draining LN HEVs, where they may have a profound impact on leukocyte recruitment. Further research will be needed to understand this complex relationship between PLNs and their micro- and macroenvironment.

We would like to thank Kristel Maijwee for excellent help during preliminary experiments, Guiying Cheng and Brian Fors for expert technical assistance, and Drs. Eugene Butcher and Aaron Warnock (Stanford University, Stanford, CA) for mAbs.

This work was supported by National Institutes of Health grants HL54936 and HL56949 and by a generous donation from Pfizer, Inc.

Submitted: 1 June 1999
Revised: 17 August 1999
Accepted: 28 September 1999

References

1. Gowans, J.L., and E.J. Knight. 1964. The route of re-circulation of lymphocytes in the rat. *Proc. R. Soc. Lond. Ser. B.* 159: 257–282.
2. Springer, T.A. 1994. Traffic signals for lymphocyte recirculation and leukocyte emigration: the multi-step paradigm. *Cell.* 76:301–314.
3. Butcher, E.C., and L.J. Picker. 1996. Lymphocyte homing and homeostasis. *Science.* 272:60–66.
4. Mondino, A., A. Khoruts, and M.K. Jenkins. 1996. The anatomy of T-cell activation and tolerance. *Proc. Natl. Acad. Sci. USA.* 93:2245–2252.
5. Catalina, M.D., M.C. Carroll, H. Arizpe, A. Takashima, P. Estess, and M.H. Siegelman. 1996. The route of antigen entry determines the requirement for L-selectin during immune responses. *J. Exp. Med.* 184:2341–2351.
6. Diacovo, T.G., M.D. Catalina, M.H. Siegelman, and U.H. von Andrian. 1998. Circulating activated platelets reconstitute lymphocyte homing and immunity in L-selectin–deficient mice. *J. Exp. Med.* 187:197–204.
7. Warnock, R.A., S. Askari, E.C. Butcher, and U.H. von Andrian. 1998. Molecular mechanisms of lymphocyte homing to peripheral lymph nodes. *J. Exp. Med.* 187:205–216.
8. Berg, E.L., M.K. Robinson, R.A. Warnock, and E.C. Butcher. 1991. The human peripheral lymph node vascular

Downloaded from http://rupress.org/jem/article-pdf/191/1/61/1123529/99-0903.pdf by guest on 24 May 2022

addressin is a ligand for LECAM-1, the peripheral lymph node homing receptor. *J. Cell Biol.* 114:343–349.
9. Streeter, P.R., B.T.N. Rouse, and E.C. Butcher. 1988. Immunohistologic and functional characterization of a vascular addressin involved in lymphocyte homing into peripheral lymph nodes. *J. Cell Biol.* 107:1853–1862.
10. von Andrian, U.H. 1996. Intravital microscopy of the peripheral lymph node microcirculation in mice. *Microcirculation.* 3:287–300.
11. Gallatin, W.M., I.L. Weissman, and E.C. Butcher. 1983. A cell-surface molecule involved in organ-specific homing of lymphocytes. *Nature.* 304:30–34.
12. Arbonès, M.L., D.C. Ord, K. Ley, H. Ratech, C. Maynard-Curry, G. Otten, D.J. Capon, and T.F. Tedder. 1994. Lymphocyte homing and leukocyte rolling and migration are impaired in L-selectin-deficient mice. *Immunity.* 1:247–260.
13. Hamann, A., D.J. Westrich, A. Duijvestijn, E.C. Butcher, H. Baisch, R. Harder, and H.G. Thiele. 1988. Evidence for an accessory role of LFA-1 in lymphocyte-high endothelium interaction during homing. *J. Immunol.* 140:693–699.
14. Andrew, D.P., J.P. Spellberg, H. Takimoto, R. Schmits, T.W. Mak, and M.M. Zukowski. 1998. Transendothelial migration and trafficking of leukocytes in LFA-1-deficient mice. *Eur. J. Immunol.* 28:1959–1969.
15. Berlin-Rufenbach, C., F. Otto, M. Mathies, J. Westermann, M.J. Owen, A. Hamann, and N. Hogg. 1999. Lymphocyte migration in lymphocyte function–associated (LFA)-1–deficient mice. *J. Exp. Med.* 189:1467–1478.
16. Stewart, M., and N. Hogg. 1996. Regulation of leukocyte integrin function: affinity vs. avidity. *J. Cell. Biochem.* 61: 554–561.
17. Spangrude, G.J., B.A. Braaten, and R.A. Daynes. 1984. Molecular mechanisms of lymphocyte extravasation. I. Studies of two selective inhibitors of lymphocyte recirculation. *J. Immunol.* 132:354–362.
18. Rollins, B.J. 1997. Chemokines. *Blood.* 90:909–928.
19. Kim, C.H., and H.E. Broxmeyer. 1999. Chemokines: signal lamps for trafficking of T and B cells for development and effector function. *J. Leukoc. Biol.* 65:6–15.
20. Tanabe, S., Z. Lu, Y. Luo, E.J. Quackenbush, M.A. Berman, L.A. Collins-Racie, S. Mi, C. Reilly, D. Lo, K.A. Jacobs, and M.E. Dorf. 1997. Identification of a new mouse β-chemokine, TCA-4, with activity on T lymphocytes and mesangial cells. *J. Immunol.* 159:5671–5679.
21. Hedrick, J.A., and A. Zlotnik. 1997. Identification and characterization of a novel β chemokine containing six conserved cysteines. *J. Immunol.* 159:1589–1593.
22. Gunn, M.D., K. Tangemann, C. Tam, J.G. Cyster, S.D. Rosen, and L.T. Williams. 1998. A chemokine expressed in lymphoid high endothelial venules promotes the adhesion and chemotaxis of naive T lymphocytes. *Proc. Natl. Acad. Sci. USA.* 95:258–263.
23. Nagira, M., T. Imai, K. Hieshima, J. Kusuda, M. Ridanpaa, S. Takagi, M. Nishimura, M. Kakizaki, H. Nomiyama, and O. Yoshie. 1997. Molecular cloning of a novel human CC chemokine secondary lymphoid-tissue chemokine that is a potent chemoattractant for lymphocytes and mapped to chromosome 9p13. *J. Biol. Chem.* 272:19518–19524.
24. Campbell, J.J., E.P. Bowman, K. Murphy, K.R. Youngman, M.A. Siani, D.A. Thompson, L. Wu, A. Zlotnik, and E.C. Butcher. 1998. 6-C-kine (SLC), a lymphocyte adhesion-triggering chemokine expressed by high endothelium, is an agonist for the MIP-3beta receptor CCR7. *J. Cell Biol.* 141: 1053–1059.
25. Yoshida, R., M. Nagira, M. Kitaura, N. Imagawa, T. Imai, and O. Yoshie. 1998. Secondary lymphoid-tissue chemokine is a functional ligand for the CC chemokine receptor CCR7. *J. Biol. Chem.* 273:7118–7122.
26. Yoshida, R., M. Nagira, T. Imai, M. Baba, S. Takagi, Y. Tabira, J. Akagi, H. Nomiyama, and O. Yoshie. 1998. EBI1-ligand chemokine (ELC) attracts a broad spectrum of lymphocytes: activated T cells strongly up-regulate CCR7 and efficiently migrate toward ELC. *Int. Immunol.* 10:901–910.
27. Ngo, V.N., H.L. Tang, and J.G. Cyster. 1998. Epstein-Barr virus–induced molecule 1 ligand chemokine is expressed by dendritic cells in lymphoid tissues and strongly attracts naive T cells and activated B cells. *J. Exp. Med.* 188:181–191.
28. Campbell, J.J., J. Hedrick, A. Zlotnik, M.A. Siani, D.A. Thompson, and E.C. Butcher. 1998. Chemokines and the arrest of lymphocytes rolling under flow conditions. *Science.* 279:381–384.
29. Tangemann, K., M.D. Gunn, P. Giblin, and S.D. Rosen. 1998. A high-endothelial cell derived chemokine induces rapid, efficient, and subset-specific arrest of rolling T lymphocytes on a reconstituted endothelial substrate. *J. Immunol.* 161:6330–6337.
30. Pachynski, R.K., S.W. Wu, M.D. Gunn, and D.J. Erle. 1998. Secondary lymphoid-tissue chemokine (SLC) stimulates integrin α4β7-mediated adhesion of lymphocytes to mucosal addressin cell adhesion molecule-1 (MAdCAM-1) under flow. *J. Immunol.* 161:952–956.
31. Nakano, H., T. Tamura, T. Yoshimoto, H. Yagita, M. Miyasaka, E.C. Butcher, H. Nariuchi, T. Kakiuchi, and A. Matsuzawa. 1997. Genetic defect in T lymphocyte-specific homing into peripheral lymph nodes. *Eur. J. Immunol.* 27:215–221.
32. Nakano, H., S. Mori, H. Yonekawa, H. Nariuchi, A. Matsuzawa, and T. Kakiuchi. 1998. A novel mutant gene involved in T-lymphocyte-specific homing into peripheral lymphoid organs on mouse chromosome 4. *Blood.* 91:2886–2895.
33. Gunn, M.D., S. Kyuwa, C. Tam, T. Kakiuchi, A. Matsuzawa, L.T. Williams, and H. Nakano. 1999. Mice lacking expression of secondary lymphoid organ chemokine have defects in lymphocyte homing and dendritic cell localization. *J. Exp. Med.* 189:451–460.
34. Sanchez-Madrid, F., P. Simon, S. Thompson, and T.A. Springer. 1983. Mapping of antigenic and functional epitopes on the alpha and beta subunits of two related glycoproteins involved in cell interactions, LFA-1 and Mac-1. *J. Exp. Med.* 158:586–602.
35. Manjunath, N., P. Shankar, B. Stockton, P.D. Dubey, J. Lieberman, and U.H. von Andrian. 1999. A transgenic mouse model to analyze $CD8^+$ effector T cell differentiation in vivo. *Proc. Natl. Acad. Sci. USA.* 96:13932–13937.
36. von Andrian, U.H., and C. M'rini. 1998. In situ analysis of lymphocyte migration to lymph nodes. *Cell Adhes. Commun.* 6:85–96.
37. Pries, A.R. 1988. A versatile video image analysis system for microcirculatory research. *Int. J. Microcirc. Clin. Exp.* 7:327–345.
38. Stockton, B.M., G. Cheng, N. Manjunath, B. Ardman, and U.H. von Andrian. 1998. Negative regulation of T cell homing by CD43. *Immunity.* 8:373–381.
39. Sawada, S., J.D. Scarborough, N. Killeen, and D.R. Littman. 1994. A lineage-specific transcriptional silencer regulates CD4 gene expression during T lymphocyte development. *Cell.* 77:917–929.
40. Oberlin, E., A. Amara, F. Bachelerie, C. Bessia, J.-L. Vireliz-

Downloaded from http://rupress.org/jem/article-pdf/191/1/61/1123529/99-0903.pdf by guest on 24 May 2022

ier, A. Arenzana-Seisdedos, O. Schwartz, J.-M. Heard, I. Clark-Lewis, D.F. Legler, et al. 1996. The CXC chemokine, stromal cell derived factor 1 (SDF-1), is the ligand for LESTR/fusin and prevents infection by T-cell-line-adapted HIV-1. *Nature*. 382:833–835.

41. Bleul, C.C., M. Farzan, H. Choe, C. Parolin, I. Clark-Lewis, J. Sodroski, and T.A. Springer. 1996. The lymphocyte chemoattractant SDF-1 is a ligand for LESTR/fusin and blocks HIV-1 entry. *Nature*. 382:829–833.
42. Bargatze, R.F., M.A. Jutila, and E.C. Butcher. 1995. Distinct roles of L-selectin and integrins α4β7 and LFA-1 in lymphocyte homing to Peyer's patch-HEV in situ: the multistep model confirmed and refined. *Immunity*. 3:99–108.
43. Nagira, M., T. Imai, R. Yoshida, S. Takagi, M. Iwasaki, M. Baba, Y. Tabira, J. Akagi, H. Nomiyama, and O. Yoshie. 1998. A lymphocyte-specific CC chemokine, secondary lymphoid tissue chemokine (SLC), is a highly efficient chemoattractant for B cells and activated T cells. *Eur. J. Immunol.* 28: 1516–1523.
44. Miura, S., Y. Tsuzuki, D. Fukumara, H. Serizawa, M. Suematsu, I. Kurose, H. Imaeda, H. Kimura, H. Nagata, M. Tsuchiya, et al. 1995. Intravital demonstration of sequential migration process of lymphocyte subpopulations in rat Peyer's patches. *Gastroenterology*. 109:1113–1123.
45. Stevens, S.K., I.L. Weissman, and E.C. Butcher. 1982. Differences in the migration of B and T lymphocytes. Organ-selective localization in vivo and the role of lymphocyte-endothelial cell recognition. *J. Immunol.* 2:844–851.
46. Quackenbush, E J., V. Aguirre, B.K. Wershil, and J.C. Gutierrez-Ramos. 1997. Eotaxin influences the development of embryonic hematopoietic progenitors in the mouse. *J. Leukoc. Biol*. 62:661–666.
47. Yoshida, R., T. Imai, K. Hieshima, J. Kusuda, M. Baba, M. Kitaura, M. Nishimura, M. Kakizaki, H. Nomiyama, and O. Yoshie. 1997. Molecular cloning of a novel human CC chemokine EBI1-ligand chemokine that is a specific functional ligand for EBI1, CCR7. *J. Biol. Chem.* 272:13803–13809.
48. Soto, H., W. Wang, R.M. Strieter, N.G. Copeland, D.J. Gilbert, N.A. Jenkins, J. Hedrick, and A. Zlotnik. 1998. The CC chemokine 6Ckine binds the CXC chemokine receptor CXCR3. *Proc. Natl. Acad. Sci. USA*. 95:8205–8210.
49. Ma, Q., D. Jones, and T.A. Springer. 1999. The chemokine receptor CXCR4 is required for the retention of B lineage and granulocytic precursors within the bone marrow microenvironment. *Immunity*. 10:463–471.
50. Kim, C.H., L.M. Pelus, J.R. White, E. Applebaum, K. Johanson, and H.E. Broxmeyer. 1998. CKbeta-11/macrophage inflammatory protein-3beta/EBI1-ligand chemokine is an efficacious chemoattractant for T and B cells. *J. Immunol.* 160: 2418–2424.
51. Bleul, C.C., R.C. Fuhlbrigge, J.M. Casasnovas, A. Aiuti, and T.A. Springer. 1996. A highly efficacious lymphocyte chemoattractant, stromal cell–derived factor 1 (SDF-1). *J. Exp. Med.* 184:1101–1110.
52. Girard, J.-P., and T.A. Springer. 1995. High endothelial venules (HEVs): specialized endothelium for lymphocyte migration. *Immunol. Today*. 16:449–457.
53. Middleton, J., S. Neil, J. Wintle, I. Clark-Lewis, H. Moore, C. Lam, M. Auer, E. Hub, and A. Rot. 1997. Transcytosis and surface presentation of IL-8 by venular endothelial cells. *Cell*. 91:1001–1011.
54. Rot, A. 1992. Endothelial cell binding of NAP-1/IL-8: role in neutrophil emigration. *Immunol. Today*. 13:291–294.
55. Tanaka, Y., D.H. Adams, S. Hubscher, H. Hirano, U. Siebenlist, and S. Shaw. 1993. T-cell adhesion induced by proteoglycan-immobilized cytokine MIP-1beta. *Nature.* 361:79–82.
56. Hub, E., and A. Rot. 1998. Binding of RANTES, MCP-1, MCP-3, and MIP-1α to cells in human skin. *Am. J. Pathol.* 152:749–757.
57. Anderson, A.O., and S. Shaw. 1993. T cell adhesion to endothelium: the FRC conduit system and other anatomic and molecular features which facilitate the adhesion cascade in lymph node. *Semin. Immunol.* 5:271–282.
58. Gretz, J.E., E.P. Kaldjian, A.O. Anderson, and S. Shaw. 1996. Sophisticated strategies for information encounter in the lymph node. *J. Immunol*. 157:495–499.
59. Wagner, L., O.O. Yang, E.A. Garcia-Zepeda, Y. Ge, S.A. Kalams, B.D. Walker, M.S. Pasternack, and A.D. Luster. 1998. β-chemokines are released from HIV-1-specific cytolytic T-cell granules complexed to proteoglycans. *Nature*. 391:908–911.
60. Hendriks, H.R., and I.L. Eestermans. 1983. Disappearance and reappearance of high endothelial venules and immigrating lymphocytes in lymph nodes deprived of afferent lymphatic vessels: a possible regulatory role of macrophages in lymphocyte migration. *Eur. J. Immunol.* 13:663–669.
61. Hendriks, H.R., A.M. Duijvestijn, and G. Kraal. 1987. Rapid decrease in lymphocyte adherence to high endothelial venules in lymph nodes deprived of afferent lymphatic vessels. *Eur. J. Immunol*. 17:1691–1695.
62. Mebius, R.E., P.R. Streeter, J. Breve, A.M. Duijvestijn, and G. Kraal. 1991. The influence of afferent lymphatic vessel interruption on vascular addressin expression. *J. Cell Biol*. 115: 85–95.
63. Tedla, N., H.W. Wang, H.P. McNeil, N. DiGirolamo, T. Hampartzoumain, D. Wakefield, and A. Lloyd. 1998. Regulation of T lymphocyte trafficking into lymph nodes during an immune response by the chemokines macrophage inflammatory protein (MIP)-1α and MIP-1β. *J. Immunol*. 161: 5663–5672.
64. Vassileva, G., H. Soto, A. Zlotnik, H. Nakano, T. Kakiuchi, J.A. Hedrick, and S.A. Lira. 1999. The reduced expression of 6Ckine in the *plt* mouse results from the deletion of one of two 6Ckine genes. *J. Exp. Med.* 190:1183–1188.

Downloaded from http://rupress.org/jem/article-pdf/191/1/61/1123529/99-0903.pdf by guest on 24 May 2022